

Power Quality Monitoring and Control for DFIG Wind Generation

Suratsavadee K. Korkua
Student Member, IEEE,

Wei-Jen Lee
Fellow, IEEE

Hung-Chi Chen
Member, IEEE

Abstract-- As wind power is growing towards becoming a major utility source, it is urgent to guarantee the reliable operation of wind power systems. The power quality monitoring system for wind turbine based on vibration analysis is studied. The rotor imbalance is successfully detected by using machine vibration analysis. Moreover, the systematic control design of the proposed vibration suppression by means of a rotor side inverter controller is explored and discussed. The real wind speed data of three different cases from the ERCOT system were used as input to test the performance and capabilities of the control scheme. The simulation results of the generator output show the effectiveness of this proposed rotor side inverter controller. It effectively reduces the oscillation of power output of the DFIG wind turbine.

Index Terms-- Doubly-fed induction generator (DFIG), monitoring, wind turbine, rotor side inverter

I. INTRODUCTION

THE wind energy industry has developed rapidly through the last 10-20 years. Factories have gone from small-scale operations to a mature industry, and from a technical standpoint, wind turbines have increased in size, reduced in cost, and improved in the controllability. This makes modern wind energy a serious and competitive alternative to other energy sources.

The development has been concentrated on wind turbine systems for electrical power production, i.e. grid-connected wind turbines. Grid-connected wind turbines are a part of a power system with which they interact. The power system and its quality have an influence on the wind turbines' performance, lifetime, and safety. Therefore, the integration of wind power into the power systems has become an important issue in development and research of wind power [1-2].

To avoid unexpected equipment failures, the focus in most wind farm is shifting from scheduled preventive maintenance to predictive maintenance. Predictive maintenance by condition-based monitoring of electrical machines is a scientific approach that is becoming a new strategy for maintenance management. Machine vibration analysis is also a measurement tool used to identify, predict, and prevent failures in rotating machinery. Implementing vibration

analysis will improve the reliability of the machine and lead to better monitoring power output, reducing downtime by eliminating unexpected mechanical or electrical failures.

Moreover, to improve the quality of wind turbine output and to suppress the vibration on the rotating part of the machine during the rotor imbalance condition, the doubly-fed induction generator (DFIG) wind turbine control system is studied and a new control strategy for the rotor side inverter controller to suppress the power fluctuation due to rotor imbalance of the wind turbine is also proposed. Under the wind turbine control level, the oscillating rotor side current is first extracted by frequency-varying low bandwidth band-pass filter. This rotor current is then used to estimate the next sampling stator side current in order to better perform the current control. The stator flux amplitude and phase angle are also estimated during the rotor imbalance condition. Modification of decoupling voltage control makes it possible to obtain the estimated rotor voltage that is needed to inject the desired current into the DFIG via the current-controlled voltage source PWM inverter. This technique reduces the oscillation of wind turbine output by control from the rotor side, which requires lower power injection compared with the grid side converter; furthermore, no extra hardware is required. The feasibility of this design has been proven by means of mathematical model and digital simulations based on Matlab/Simulink. The simulation results of the generator output show the effectiveness of this proposed rotor side inverter controller.

II. WIND TURBINE MONITORING SYSTEM

Analysis of wind farm maintenance costs has shown that up to 40% of the cost can be related to unexpected failures of wind turbine components that then lead to unscheduled corrective maintenance actions [3-4]. A wind turbine consists of thousands of components and is subject to different sorts of failures. Some of them are more frequent than others but in order to compare among them it is necessary to consider the downtime they could force for the whole system.

Reference [5] shows the annual average downtimes of major wind turbine subassemblies according to the LWK survey of more than 2000 wind turbines for 11 years. It is seen that gearbox, electrical system, rotor blade, and generator are ranked the four most critical subassemblies based on annual average downtime; consequently, they should received the highest priority for monitoring due to the high downtime caused by their malfunction.

S. K. Korkua and W. J. Lee are with the Department of Electrical Engineering, the University of Texas at Arlington (UTA), TX 76013 USA (e-mail: ksuratsavadee@yahoo.com and wlee@uta.edu).

H. C. Chen is with the Department of Electrical Engineering, National Chiao Tung University (NCTU), Hsinchu, Taiwan (e-mail: hcchen@cn.nctu.edu.tw).

In this work, we mainly focus on the monitoring of wind turbines, as mechanical components account for the majority of wind turbine equipment, and vibration monitoring is thus a key component of this condition based monitoring system. The vibration signals carry information about structural resonance and other components in the machine by means of vibration transducer. When the machine is in good condition and is running under normal operating conditions, it produces a certain vibration pattern specific to its vibration behavior and character, but as degradation starts in, the characteristics of the vibration signals changes. The goal for this research is not only to monitor the machine health of wind turbine system, but also to develop a control method for doubly-fed induction generators (DFIG) that addresses the issues associated to the rotor imbalance condition of the generator.

Rotor imbalance is a mechanical disturbance related problem. It is a condition where there is more weight distributed on one side of a rotating part of the rotor than on the other side. It might be caused by wind wheel unbalances, shaft imbalances, or mechanical looseness. This kind of event will directly cause oscillation on the output signal of the generator such as generated output power, current, and voltage.

A. Vibration Sensor Equipment

In the wind power industry, vibration monitoring is used primarily to detect faults in mechanical components such as the bearings and gears installed inside the wind turbine nacelle. Modern type wind turbines are mainly based on rotational components. Therefore, measurement of vibration on component housings and structural oscillation will yield data for calculating characteristic values by means of advanced condition monitoring and fault prediction algorithms. Figure 1 shows a possible configuration of sensors installed on the drive train [6]. The type of sensor depends more or less on the frequency range relevant for the monitoring.

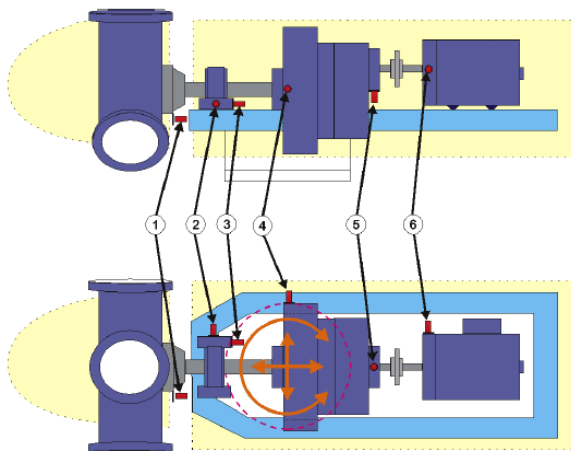


Fig. 1. Common Sensor Configurations for Wind Turbine

The mounting positions of the sensors are indicated with labels 2, 3 and 4. These positions allow the measurement of

the nacelle oscillation modes. For monitoring of the gearbox, bearing, and generator conditions, the vibration sensors operating at a frequency range from 1 Hz to 20,000 Hz will be used to measure the vibration induced by gearwheels, bearings, and rotating part of generators. Labels 5 and 6 show an example for the position of the gearbox and generator vibration sensors.

B. Machine Vibration Analysis

Using vibration analysis, the presence of a failure, or even an upcoming failure, can be detected because of the increase or modification in vibrations of industrial equipment. Since an analysis of vibrations is a powerful tool for the diagnosis of equipment, a number of different techniques have been developed. In general, there are two main approaches used for processing the signal: time domain and frequency domain. It is important to use the method that is best suited for each particular piece of equipment.

Implementation of Root Mean Square

The RMS value of the vibration signal is used for primary investigation of the machine health. The RMS values will be used to detect the severity of the abnormal condition. These values could also be used as input to training the neural network based fault classifier.

Implementation of Crest factor

The crest factor is the ratio of the peak value of the vibration signal to the RMS value. The purpose of the crest factor calculation is to give the analyst a quick idea of how much impacting is occurring in a waveform. It is meaningful where the peak values are reasonably uniform and repetitive from one cycle to another. Crest factor is often used to indicate faults in the rolling element bearings. The values of the crest factor of the vibration signal in the healthy case will be used as a baseline condition in monitoring system. Using both the RMS value and the crest factor for the machine health diagnostic may increase the overall system performance for health monitoring systems.

Implementation of Spectrum Analysis

The Fast Fourier Transform (FFT) algorithm is used to extract some useful features of the vibration signal, and the set of frequency components related to different types of faults can thus be obtained. In order to achieve the earliest possible recognition of a fault in the machine, a comparison of the spectrum of the machine with the spectrum of the healthy case must be performed. The amplitudes of the frequency components can be used to specify the degree of fault for various operating conditions.

The vibration signal information will be sampled and stored in the computer memory. Both the time domain and frequency domain approach will be used to obtain the machine's health condition. All the techniques mentioned here for signal analysis and processing can be implemented by MATLAB software. Based on the vibration spectrum analysis, it is normally straightforward to locate the mechanical rotational frequency by monitoring the vibration spectrum and finding the most significant peak in the expected rotational frequency

range. This peak amplitude at the rotational frequency serves as the rotor imbalance indicator for the monitoring system. Furthermore, the amplitude of this frequency component reveals the severity level of the rotor imbalance fault [7-9]. A block diagram of the proposed severity detection of rotor imbalance is shown in Figure 2.

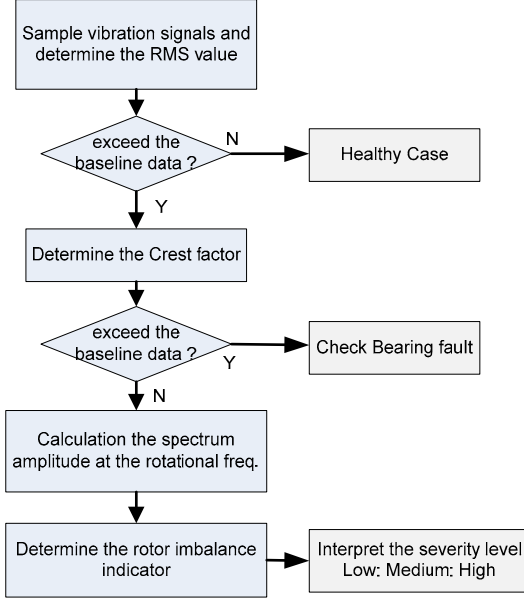


Fig. 2. Mechanical vibration analysis for wind turbine monitoring system

III. OPERATION OF WIND GENERATION SYSTEM

A. Overall Control System of DFIG

In this study, the overall control structure of the wind turbine system consists of an aerodynamic model, a transmission system, a generator model, a DFIG control level block model, and a wind turbine control level block model [10]. As shown in Fig. 3, the stator of the DFIG is connected directly to the incoming AC mains, whereas the wound rotor is fed from the power electronics converter through slip rings. The DC link capacitor that connects the stator and rotor side inverters stores the power obtained from the induction generator for further generation usage.

A wind turbine control level provides reference signals both to the pitch system of the wind turbine and to the DFIG control level. It contains two controllers: Power Controller and Pitch Controller. It generates the active power reference signal for the active power control loop, performed by the rotor side inverter controller in the DFIG control level. A DFIG control level contains the electrical control of the power converters and of the doubly-fed induction generator with a fast dynamic response. It contains two controllers: Grid side converter controller and Rotor side inverter controller.

B. Doubly Fed Induction Generator Model

Using Park's transformation from stationary reference frame to rotating reference frame, the dynamic model for a wound rotor induction machine (DFIG) is defined as follows [11]:

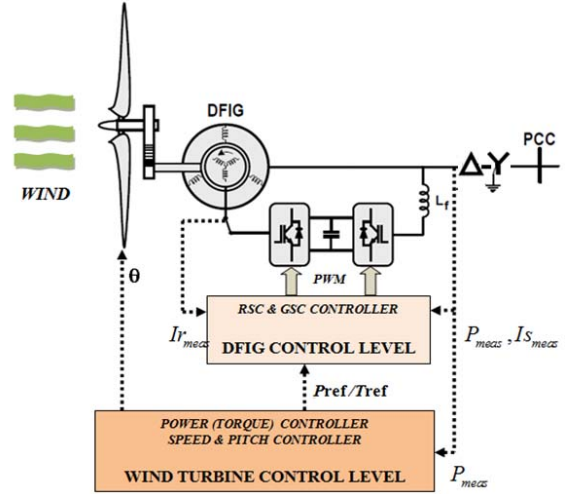


Fig. 3 Configuration of a DFIG wind turbine

Stator voltage equations:

$$V_{sd} = p\lambda_{sd} - \omega\lambda_{sq} + R_s i_{sd} \quad (1)$$

$$V_{sq} = p\lambda_{sq} + \omega\lambda_{sd} + R_s i_{sq}$$

Rotor voltage equations:

$$V_{rd} = p\lambda_{rd} - (\omega - \omega_r)\lambda_{rq} + R_r i_{rd} \quad (2)$$

$$V_{rq} = p\lambda_{rq} + (\omega - \omega_r)\lambda_{rd} + R_r i_{rq}$$

Stator flux equations:

$$\lambda_{sd} = (L_{ls} + L_m)i_{sd} + L_m i_{rd} \quad (3)$$

$$\lambda_{sq} = (L_{ls} + L_m)i_{sq} + L_m i_{rq}$$

Rotor flux equations:

$$\lambda_{rd} = (L_{lr} + L_m)i_{rd} + L_m i_{sd} \quad (4)$$

$$\lambda_{rq} = (L_{lr} + L_m)i_{rq} + L_m i_{sq}$$

The electromagnetic torque, the power and reactive power equations may be written as:

$$T_s = -\frac{3}{2}p(\lambda_{sd}i_{sq} - \lambda_{sq}i_{sd}) \quad (5)$$

$$P_s = \frac{3}{2}(V_{sd}i_{sd} + V_{sq}i_{sq})$$

$$Q_s = \frac{3}{2}(V_{sq}i_{sd} - V_{sd}i_{sq})$$

IV. THE PROPOSED ROTOR SIDE INVERTER CONTROLLER

The proposed method intends to design a control strategy using the rotor side inverter to help reduce the oscillation of the wind turbine's output when rotor imbalance affects the generator. The current control approach considering a vector oriented control (VOC) philosophy in the d-q reference frame is applied. The rotor side inverter controls independently the active and reactive power. The power is controlled indirectly by controlling the rotor current. In this control scheme, the rotor side inverter is controlled in a synchronously rotating d-q axis reference frame, with the d-axis oriented along the stator-flux vector position as shown in Fig. 4. In this way, a decoupled control between the electrical torque and the rotor excitation current is also obtained [12].

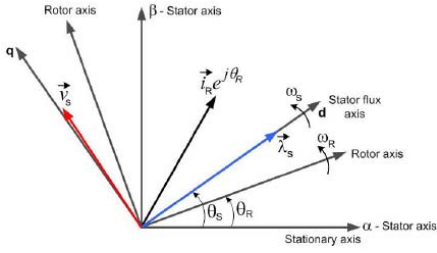


Fig. 4. Vector Diagram in a Field Oriented Control

The layout of the proposed control structure of the rotor side inverter controller is shown in Fig. 5. The current control approach considering a vector oriented control (VOC) philosophy in the d-q reference frame is applied. As depicted in Fig. 5, under normal power-speed control from wind turbine control level and combining the stator flux amplitude/phase angle estimator with oscillating current extraction, the current components at the oscillating frequency were extracted. This rotor current is also used to estimate the next sampling stator side current in order to better perform the current control. Modification of decoupling voltage control makes it possible to obtain the estimated rotor voltage that is needed to inject the desired current into the DFIG via the current-controlled voltage source PWM inverter.

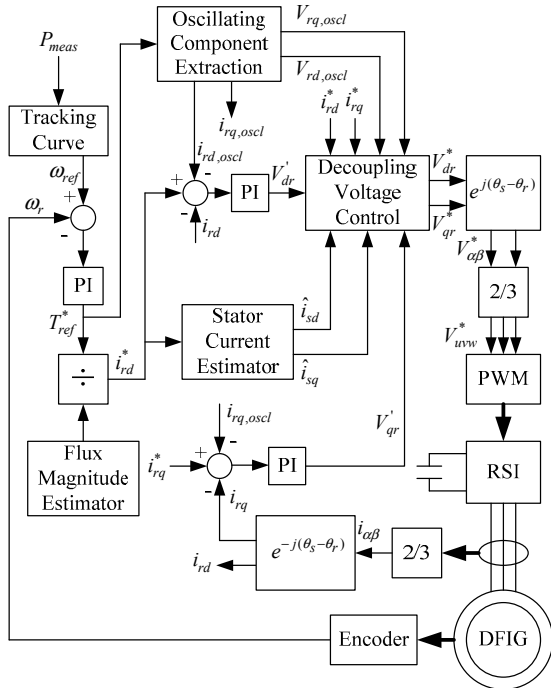


Fig. 5. Proposed control structure of the rotor side inverter controller

A. Stator Flux Magnitude and Phase Angle Estimation

From the coordinate of stator flux on d-q reference frame, the expression of the stator flux magnitude ($|\lambda_s|$) can be defined as

$$\begin{aligned} \lambda_{sd} &= \int (V_{sd} - R_s i_{sd}) dt \\ \lambda_{sq} &= \int (V_{sq} - R_s i_{sq}) dt \\ |\lambda_s| &= \sqrt{(\lambda_{sd})^2 + (\lambda_{sq})^2} \end{aligned} \quad (6)$$

The phase angle (θ_e) is calculated by

$$\theta_e = \tan^{-1} \frac{\lambda_{sq}}{\lambda_{sd}} \quad (7)$$

B. Oscillating Rotor Current Extraction

In order to keep all other frequency current components, the frequency-varying band-pass filter is used to extract only the oscillating current component at a particular frequency. This will come to effect only in the presence of the rotor imbalance. It is designed to have large gain at the known disturbance frequency (oscillating frequency) but also have a negligible effect at all other frequencies. The oscillating frequency can be determined by the fault detection. The harmonics of rotor imbalance can be modeled as an integer multiple of rotating frequency [13]:

$$f_{vib} = k \cdot \left[f_s \left(\frac{1-s}{P} \right) \right] \quad (8)$$

where f_s is stator side frequency, k is the integer number, P is the number of pole pair, and s is the slip.

This current extraction is done by using a high-Q second order band-pass filter. For a second-order low bandwidth band-pass filter the transfer function is given by

$$H(s) = \frac{H_0 \beta s}{s^2 + \beta s + \omega_0^2} \quad (9)$$

where β is Bandwidth, $\omega_0 = 2\pi f_0$ is Center/Natural frequency, H_0 is Maximum amplitude of the filter

C. Stator Side Current Estimation

Since the aim of this research is to suppress the vibration which causes the harmonics at a certain frequency of stator current, this event is considered as one kind of disturbance. In order to operate this proposed rotor side inverter controller during this event, the stator side current estimator is integrated into this controller. The objective of this part will be focused on finding a relationship between the state space variables that could permit prediction of the behavior of the DFIG under disturbance conditions.

The current estimator will predict the dynamic stator current in a d-q rotating reference frame by estimating the stator current vector from the rotor side current vector [14]. The predicted output response of the stator current should be closed to the real stator current and should have fast dynamic response. Once the stator current vector is correctly estimated by calculating from the rotor side current vector, any unwanted signal due to disturbance can be suppressed by applying proper controlling signals from the rotor side inverter.

First, considering that the dynamic voltage equation of the rotor is linear and assuming that the magnetic circuit of DFIG is linear, by applying the Laplace transformation, we can obtain the stator current on the d-q rotating frame as follows;

$$\begin{aligned} i_{sd} &= \frac{(L_s s + R_s) V_{sd} + \omega_s L_s V_{sq}}{L_s^2 s^2 + 2L_s R_s s + R_s^2 + \omega_s^2 L_s^2} - \frac{(L_s s^2 + R_s s + \omega_s^2 L_s) L_m i_{rd} - R_s \omega_s L_m i_{rq}}{L_s^2 s^2 + 2L_s R_s s + R_s^2 + \omega_s^2 L_s^2} \\ i_{sq} &= \frac{(L_s s + R_s) V_{sq} - \omega_s L_s V_{sd}}{L_s^2 s^2 + 2L_s R_s s + R_s^2 + \omega_s^2 L_s^2} - \frac{(L_s s^2 + R_s s + \omega_s^2 L_s) L_m i_{rq} + R_s \omega_s L_m i_{rd}}{L_s^2 s^2 + 2L_s R_s s + R_s^2 + \omega_s^2 L_s^2} \end{aligned} \quad (10)$$

By considering that the stator flux is aligned with the d-q reference frame in a field oriented control system, and hence its quadrature component is zero. Assuming that the leakage inductance is low, the stator voltage vector can be considered to be almost aligned with the q-axis. Therefore, in the steady state, the current in the stator windings can be written as:

$$\begin{aligned} i_{sd} &= \frac{1}{\omega_s L_s} V_{sq} - \frac{L_m}{L_s} i_{rd} \\ i_{sq} &= \frac{R_s}{\omega_s^2 L_s^2} V_{sq} - \frac{L_m}{L_s} i_{rq} \end{aligned} \quad (11)$$

From the above equation, since the inductive reactance is much greater than the stator resistance it can be concluded that the stator's voltage term tends to zero. This equation can be reduced and the predicted stator current on d-q component as shown below:

$$\begin{aligned} \hat{i}_{sd} &= \frac{1}{\omega_s L_s} V_{sq} - \frac{L_m}{L_s} i_{rd} \\ \hat{i}_{sq} &= -\frac{L_m}{L_s} i_{rq} \end{aligned} \quad (12)$$

D. Modified Decoupling Voltage Control

The aim of this analysis is to control the d-q current components carried out for the rotor side inverter. Using a stator flux-oriented approach, implementation with the current-controlled PWM converter requires a decoupling control scheme [15].

By defining the leakage factor of the induction machines as

$$\sigma = 1 - \frac{L_m^2}{(L_{ls} + L_m)(L_{lr} + L_m)} \quad (13)$$

Substituting this leakage factor equation into rotor flux equations:

$$\begin{aligned} \lambda_{rd} &= \sigma L_s i_{rd} + \frac{L_m}{L_s} \lambda_{sd} \\ \lambda_{rq} &= \sigma L_r i_{rq} \end{aligned} \quad (14)$$

Applying these flux equations and rearranging the d-q rotor voltage equations, we obtain the following:

$$\begin{aligned} V_{rd} &= R_r i_{rd} + \sigma L_r \frac{di_{rd}}{dt} - \omega_{slip} \sigma L_r i_{rq} \\ V_{rq} &= R_r i_{rq} + \sigma L_r \frac{di_{rq}}{dt} + \omega_{slip} (\sigma L_m i_{ms} + \sigma L_r i_{rd}) \end{aligned} \quad (15)$$

The current errors on both d-q components are processed by PI controller to give V'_{rd} , and V'_{rq} respectively. This voltage output can be formed as follow;

$$\begin{aligned} V'_{rd} &= R_r i_{rd} + \sigma L_r \frac{di_{rd}}{dt} \\ V'_{rq} &= R_r i_{rq} + \sigma L_r \frac{di_{rq}}{dt} \end{aligned} \quad (16)$$

Since this system needs to adapt to disturbance condition and we want to ensure good tracking of the current control with fast dynamic response, the above decoupling voltage equations need to be modified. In order to perform a better current control and obtain a more accurate reference voltage command, the compensation terms are added to the reference voltages, making it possible to achieve decoupled

performance of stator flux-oriented control of rotor side inverter controller. The predicted stator current which estimated from rotor side current components will also be taken into account. In order to eliminate the harmonics of current components at the oscillating frequency, the compensation voltage calculated from oscillating current extraction will be added. Finally, the modified reference voltages command can be represented in these following equations;

$$\begin{aligned} V_{rd}^* &= V'_{rd} + i_{rd}^* R_r - \omega_{slip} (L_r i_{rd}^* + L_m \hat{i}_{sd}) + i_{rd_oscill} R_r \\ V_{rq}^* &= V'_{rq} + i_{rq}^* R_r + \omega_{slip} (L_r i_{rq}^* + L_m \hat{i}_{sq}) + i_{rd_oscill} \omega_{slip} L_r \end{aligned} \quad (16)$$

As mentioned, a current-controlled voltage source PWM inverter is chosen in this study. In order to control the generator current output, this inverter will force the rotor current to follow their reference signals in both on d-q reference frame via the required reference voltages (V_{rd}^* , V_{rq}^*) by injecting at the rotor windings.

V. SIMULATION SETUP AND RESULTS

The proposed control of the rotor side inverter was verified on a 9MW wind farm with GE1.5MW doubly fed induction generator (DFIG) through computer simulation. It is assumed that the DFIGs in the wind farm act coherently. All machine parameters and aerodynamic characteristic of this device are presented in Table I.

TABLE I 9-MW WIND FARM PARAMETERS IN THIS STUDY

Parameter (Unit)	Value
Nominal power (MVA)	9
Rated voltage (V)	575
Nominal frequency(Hz)	60
Stator resistance (p.u.)	0.007
Stator leakage inductance (p.u.)	0.171
Magnetizing inductance (p.u.)	2.9
Rotor resistance (p.u.)	0.005
Rotor leakage inductance (p.u.)	0.156
Number of pairs of poles	2
Nominal DC voltage (V)	1200

The system performance and capabilities of the discussed control strategy were tested under different operating conditions such as normal operation and under rotor imbalance conditions. Simulation of this proposed control strategy was carried out on MATLAB/Simulink. Three events of real wind speed were used as wind speed input; wind ramp up, wind ramp down, and a wind gust event. To perform the vibration suppression of the DFIG, the rotor imbalance condition is introduced into the wind turbine system.

A. Instantaneous Wind Ramp up Event

As shown in Fig. 6, on February 25th, 2008, the wind speed in the ERCOT system was suddenly ramped up and resulted in the wind generated power output jumping from 235 MW to 521 MW in 18 seconds. To perform the proposed control capability of rotor side inverter controller during this wind event, the rotor imbalance condition will be introduced into the system at t=5 second and the vibration suppression

scheme will later be applied at $t=10$ second.

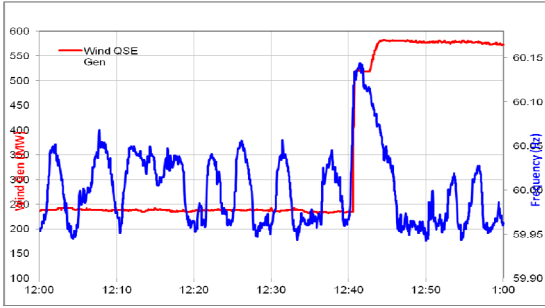


Fig. 6. Wind Ramp up Event on February 25th, 2008

The simulation results, depicted in Fig. 6, show the response of the wind speed, generator speed, generated power and torque during the wind ramp up event. When the rotor imbalance occurs at $t=5$ second, the power output and torque starts to oscillate which we can see from the zoomed version results in Fig. 7. The oscillating frequency varies due to the real wind speed. Later at $t=10$ second, vibration suppression scheme is applied. The control system takes less than 500 ms to control the current of the stator side. Fig. 8 illustrates the DFIG behavior both before and after the suppression. The stator current flowing to the grid is back to sinusoidal waveform after suppression. The simulations confirm effectiveness of the proposed scheme during the wind ramp up event.

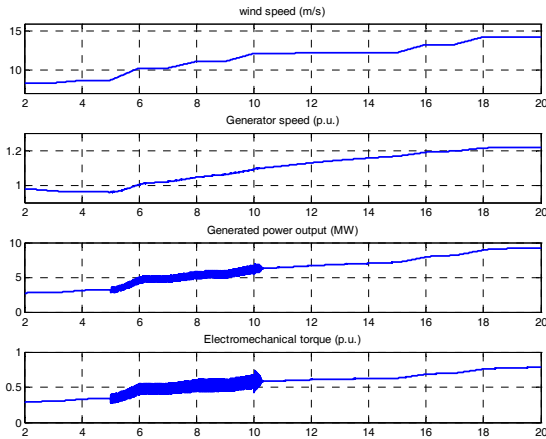


Fig. 7. Simulation Results of Wind Speed (m/s), Generator Speed (p.u.), Generated Power Output (MW) and Electromechanical Torque (p.u.) responded on Wind Ramp up Event

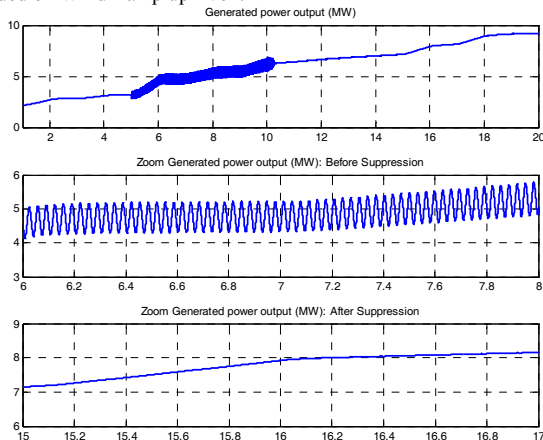


Fig. 8. Simulation Results of Generated Power Output (MW): Before and After Suppression

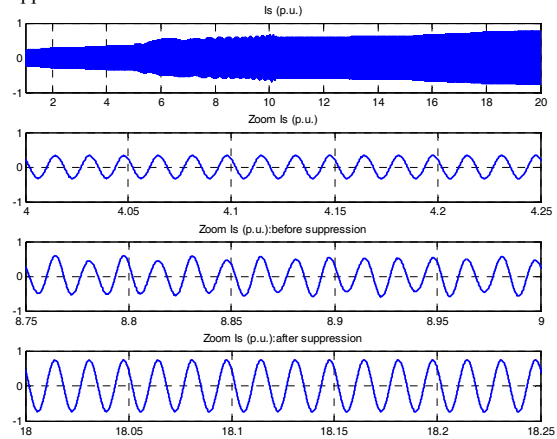


Fig. 8 Simulation Results of Generated Current Output (p.u.) and Zoomed Versions of Current Output (p.u.): Before and After Suppression

B. Instantaneous Wind Ramp down Event

As shown in Fig. 9, on February 28th, 2008, the wind speed in the ERCOT system was suddenly ramped down and resulted in a wind generated power output decrease of 243 MW in 14 seconds.

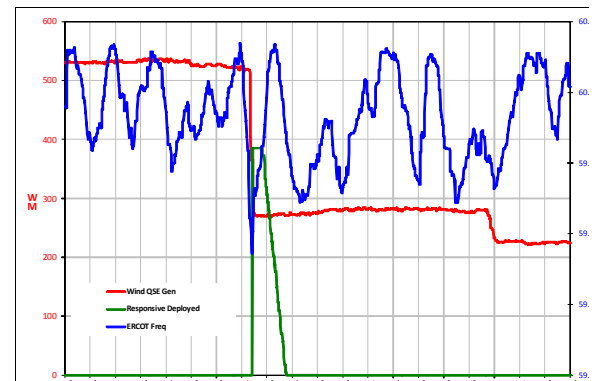


Fig. 9. Wind Ramp down Event on February 28th, 2008

The simulation results, depicted in Fig. 10, show the response of the wind speed, generator speed, generated power and torque during the wind ramp down event. Under the wind turbine control level, we can see that the wind turbine can perform following the wind speed profile.

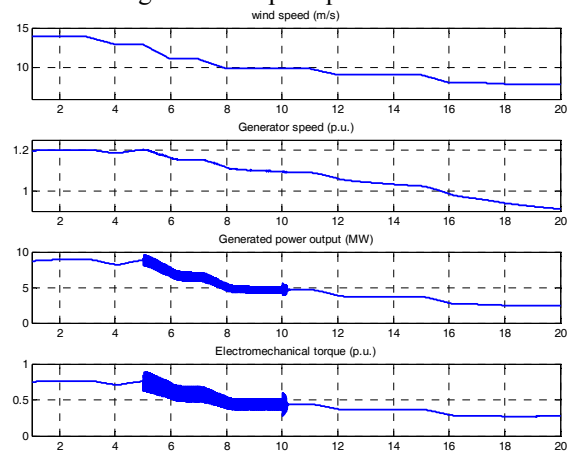


Fig. 10. Simulation Results of Wind Speed (m/s), Generator Speed (p.u.), Generated Power Output (MW) and Electromechanical Torque (p.u.)

When the rotor imbalance occurs at $t=5$ second, in Fig. 11 the power output and torque starts to oscillate which we can see. It is shown that after suppression, the stator current flowing to the grid is back to sinusoidal waveform. The simulations confirm that the proposed scheme performs well during the wind ramp down event.

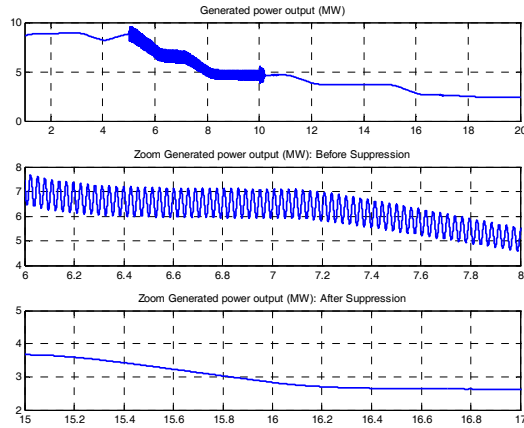


Fig. 11. Simulation Results of Generated Power Output (MW): Before and After Suppression

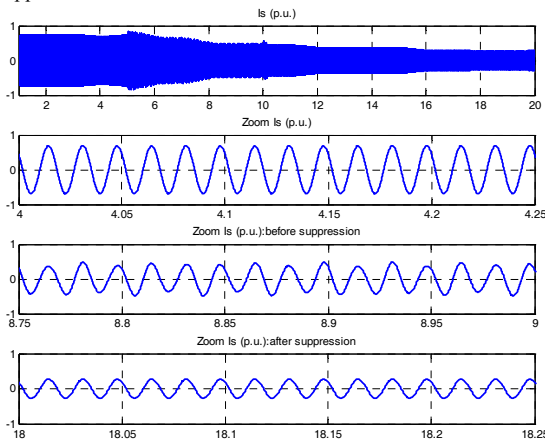
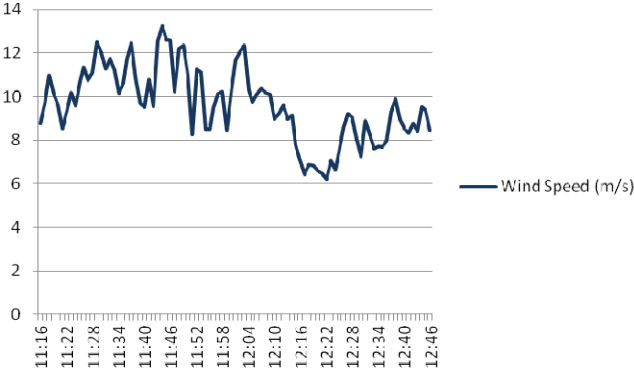


Fig. 12. Simulation Results of Generated Current Output (p.u.) and Zoomed Current Output (p.u.) Before and After Suppression

C. Wind Gust Event

As shown in Fig. 13, real wind speed data on March 4th, 2008 is used as a wind gust event input. High fluctuation of this real wind speed occurred during 11:39 PM until 12:08 AM and a 30-second time interval was selected and simulated. The minimum and maximum wind speed during this period is 8.25 m/s and 12.58 m/s, respectively.



To demonstrate the control capability of the proposed rotor side inverter controller during this wind event, the rotor imbalance condition is introduced at $t=10$ second and the vibration suppression scheme will be applied at $t=20$ second.

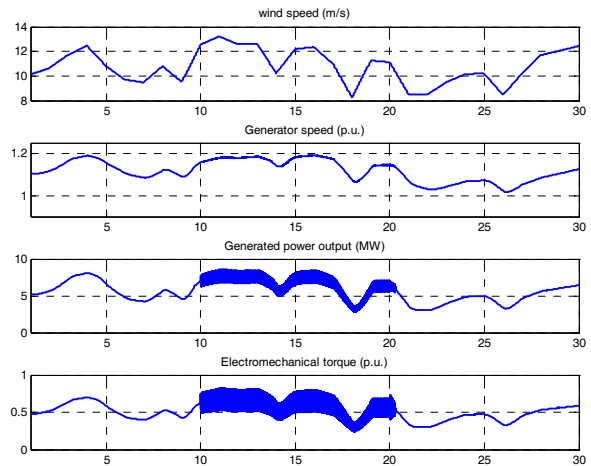


Fig. 14. Simulation Results of Wind Speed (m/s), Generator Speed (p.u.), Generated Power Output (MW) and Electromechanical Torque (p.u.)

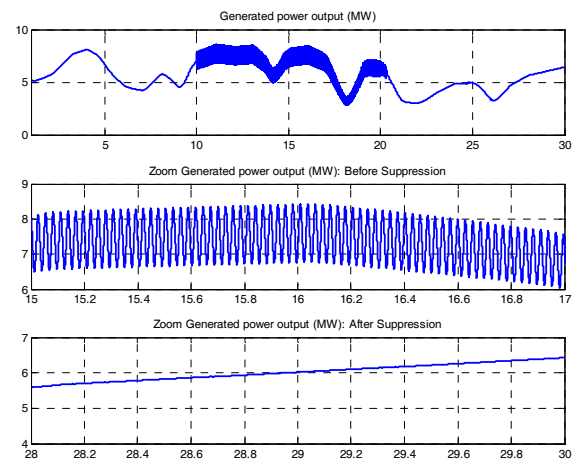


Fig. 15. Simulation Results of Generated Power Output (MW): Before and After Suppression

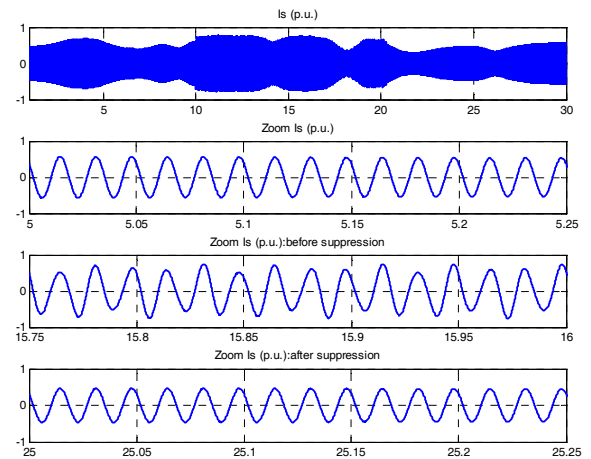


Fig. 16. Simulation Results of Generated Current Output (p.u.) and Zoomed Versions of Current Output (p.u.): Before and After Suppression

The simulation results, depicted in Fig. 14, show the response of the wind speed, generator speed, generated power and torque during the wind gust event. When the rotor imbalance occurs at $t=10$ second, the power output and torque starts to oscillate which we can see from the zoomed version results in Fig. 15. Fig. 16 illustrates the DFIG behavior both before and after suppression. At $t=21$ second after suppression, the stator current flowing to the grid is back to sinusoidal waveform. One can see that the proposed control scheme operates properly during the wind gust event.

VI. CONCLUSION

The results show that the DFIG is able to extract the maximum power by tracking the power speed characteristic. The power and torque output have the same behavior. When a rotor imbalance happens in the wind turbine system, the output signals such as power, torque and current will oscillate at the rotational frequency under traditional control scheme. This can be seen directly from the simulation results.

Once the vibration suppression scheme is introduced into the system, the oscillation of the power and current waveform is significantly improved. The ripple of active power signal also decreases. The rotor speed and generated torque show the same behavior after the suppression scheme is applied. This control takes less than 500 ms to get into the steady state region. At the steady state response region, DFIG can recovery back to normal operation where the stator current is back to sinusoidal waveform. The power output waveform show less ripple. The simulation results show the effectiveness of this proposed rotor side inverter controller.

VII. REFERENCES

- [1] W.L. Kling and J.G. Slootweg, "Wind turbines as Power Plants," in Proceedings of the IEEE/Cigré workshop on Wind Power and the Impacts on Power Systems, 17 – 18 June 2002, Oslo, Norway.
- [2] T. Burton, D. Sharpe, N. Jenkins, and E. Bossanyi, Wind Energy Handbook. John Wiley & Sons, Ltd, 2001.
- [3] M. Wilkinson, F. Spianto, M. Knowles, and P. J. Tavner, "Towards the zero maintenance wind turbine," in Proc. 41st International Universities Power Engineering Conference, vol. 1, 2006, pp.74-78.
- [4] D. McMillan and G. W. Ault, "Quantification of condition monitoring benefit for offshore wind turbines," Wind Engineering, vol. 31, no. 4, pp. 267-285, May 2007.
- [5] P.J. Tavner, G.J.W. van Bussel and F. Spinato, "Machine and converter reliabilities in wind turbines," The 3rd IET International Conference on Power Electronics, Machines and Drives, Dublin, Ireland, pp. 127-130, March 2006.
- [6] P. Caselitz and J.Giebhardt, Advanced Maintenance and Repair for Offshore Wind Farms using Fault Prediction and Condition Monitoring Techniques (OffshoreM&R). The European Commission, DG TREN
- [7] S. K. Korkua, Wei-Jen Lee, and Chiman Kwan, "Design and Implementation of ZigBee Based Vibration Monitoring and Analysis for Electrical Machines," in Proc. of the 2011 International Conference on Wireless Networks, Las Vegas, Nevada, USA, July 18-21, 2011.
- [8] S. K. Korkua, H. Jain, W. J. Lee and C. Kwan, "Detection and Severity Classification of Rotor Imbalance Faults in Induction Machines," in Proc. of 2010 IEEE Industry Applications Society Annual Meeting, Houston, Texas, USA, October 3-7, 2010.
- [9] S. K. Korkua, H. Jain, W. J. Lee and C. Kwan, "Wireless Health Monitoring System for Vibration Detection of Induction Motors," in Proc.

of the 2010 IEEE/IAS Industrial & Commercial Power Systems Technical Conference (I&CPS), Tallahassee, Florida, USA, May 9-13, 2010.

- [10] L. H. Hansen, L. Helle, F. Blaabjerg, E. Ritchie, S. Munk-Nielsen, H. Bindner, P. Sørensen, and B. Bak-Jensen, "Conceptual survey of generators and power electronics for wind turbines," Risø National Laboratory, Roskilde, Denmark, Tech. Rep. Risø-R-1205(EN), ISBN 87-550-2743-8, Dec. 2001.
- [11] P. Krause, O. Wasynczuk, and S. Sudhoff, Analysis of Electric Machinery and Drive Systems, 2nd ed. New York: IEEE Press, 2002.
- [12] R. Pena, J.C. Clare, and G. M. Asher, "Doubly fed induction generator using back-to-back PWM converters and its application to variable speed wind-energy generation," IEE Proc.-Electr. Power Appl., Vol. 143, No 3, May 1996.
- [13] C. Kral, T. G. Habetler, and R. G. Harley, "Detection of mechanical imbalances of induction machines without spectral analysis of time domain signal," IEEE Trans. Industry Applications, Vol. 40, pp.1101-1106, July, 2004.
- [14] F.K.A. Lima, A. Luna, P. Rodriguez, E.H. Watanabe, and F. Blaabjerg, "Rotor Voltage Dynamics in the Doubly Fed Induction Generator During Grid Faults", IEEE Trans. Power Electronics, vol. 25, no. 1, pp. 118-130, Jan. 2010.
- [15] F. Blaabjerg and Z. Chen, Power Electronics for Modern Wind Turbines, 1st ed.. USA: Morgan & Claypool, 2006. Subir Ray, "Electrical Power System: Concept, Theory and Practice", 2007.

VIII. BIOGRAPHIES



Suratsavadee Koonlaboon Korkua received the B.S. and M.S. degrees from the Department of Electrical Engineering, King Mongkut Institute of Technology Ladkrabang and Chulalongkorn University, Bangkok, Thailand in 2000 and 2003 respectively. Since 2004, she joined Department of the Electrical Engineering, Walailak University, Nakhon Sri Thammarat, Thailand. Currently, she is pursuing the Ph.D. degree in Department of Electrical Engineering, the University of Texas at Arlington, Arlington, TX, USA. Her research interests are power electronics, on-line, real-time equipment diagnostic and prognostic systems, advanced wireless sensors network (WSN) and renewable energy technology to improve the efficiency, reliability and safety of power system.



Wei-Jen Lee (S'85-M'85-SM'97-F'07) received the B.S. and M.S. degrees from National Taiwan University, Taipei, Taiwan, R.O.C., and the Ph.D. degree from the University of Texas, Arlington, in 1978, 1980, and 1985, respectively, all in Electrical Engineering. In 1985, he joined the University of Texas, Arlington, where he is currently a professor of the Electrical Engineering Department and the director of the Energy Systems Research Center. He has been involved in research on power flow, transient and dynamic stability, voltage stability, short circuits, relay coordination, power quality analysis, renewable energy, and deregulation for utility companies. Prof. Lee is a Fellow of IEEE and registered Professional Engineer in the State of Texas.



Hung-Chi Chen (M'06) received the B.S. and Ph.D. degrees from the Department of Electrical Engineering, National Tsing-Hua University (NTHU), Hsinchu, Taiwan, in 1996 and 2001, respectively. In 2006, he joined the Department of Electrical Engineering, National Chiao Tung University (NCTU), Hsinchu, where he is currently an Associate Professor. From September 2011, he becomes a visiting scholar in the Department of Electrical Engineering of the University of Texas at Arlington (UTA), USA.